Where To Draw the Line in Defining a Molecular Structure

Richard F. W. Bader* and Chérif F. Matta

Department of Chemistry, McMaster University, Hamilton, Ontario, L8S 4M1, Canada

Fernando Cortés-Guzmán

Departamento de Química Orgánica, Facultad de Química, Universidad Nacional Autónoma de México, Ciudad Universitaria, México D.F., México 04510

Received July 21, 2004

It is the purpose of this paper to demonstrate how the theory of atoms in molecules (AIM) can be used to complement molecular orbital models to obtain an increased understanding of molecular structure and reactivity. The oxidative addition reaction of a hydrosilane with a Mn cyclopentadienyl dicarbonyl fragment, a common constituent of a large class of organometallic complexes, provides an ideal vehicle for demonstrating the ability of AIM to not only define structure but to predict its possible instabilities, as well as recovering the rationalizations of frontier orbital theory regarding the susceptibility and mode of attack encountered in the addition reaction.

Where to Draw the Line in a Molecular Structure

At the 2003 fall meeting of the American Chemical Society in New York a paper was presented at the symposium on "Contemporary aspects of chemical bonding" entitled "Where to draw the line? Sigma bond addition to metals". The title was in reference as to how one might best describe the bonding in the adduct resulting from the reaction of $HSiCl_3$ with $Cp(CO)_2Mn$. The talk and a recent published account, both by Lichtenberger,[1] which describe the molecular orbital approach to this problem coupled with photoelectron data, favor the classical oxidative addition product structure **2** over the σ-bond complex **1**, with the possibility of some residual Si−H interaction as described in valence bond drawings **3** and **4**.

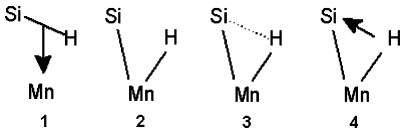

Other possible valence bond structures are considered,[2] and Lichtenberger states, "Part of the puzzle arises from the inadequacy of simple valence bond models to account for the electronic structure of organometallic molecules." It is the purpose of this paper to point out that the topology of the electron density can be used to answer the question "Where to draw the line?" and to do so in a manner that illustrates how this approach embodied in the quantum theory of atoms in molecules (QTAIM)[3] may be used to complement the orbital models employed by Lichtenberger.

Atoms, Structure, and the Electron Density

Chemistry is built on the understanding that matter is composed of atoms, with characteristic and additive properties, that are linked by bonds, an understanding that is recovered by physics. The boundary condition that leads to the definition of an atom in a molecule as an object whose properties are subject to the laws of quantum mechanics is stated in terms of the topology exhibited by the measurable charge density, the same topology yielding a criterion for bonding. The topology and structure of the density are summarized in terms of its extrema or critical points where $\nabla\rho(\mathbf{r}) = \mathbf{0}$. The interatomic surfaces satisfying the boundary condition are surfaces of zero flux, illustrated in Figure 1 by the two surfaces bounding the basin of the hydridic hydrogen in the adduct $Cp(CO)_2Mn|H|SiCl_3$. Also indicated are the two lines of maximum density, each emanating from a bond critical point (CP), that link the interior proton to the nuclei of the Si and Mn atoms. The surfaces are defined by the gradients of the density that *terminate* at a bond CP, a red dot in Figure 1, and since gradient vectors never intersect, the result is a surface with a zero flux in the gradient vectors of ρ. The bond CP also serves as the *origin* of the two unique trajectories of ρ that link the proton with the nuclei of the Si and Mn atoms. As detailed in the caption for Figure 1, a bond CP has the designation (3,−1) because two of the *three* principal curvatures of the density at the CP are negative, while the curvature of the remaining one, along the bond path, is positive, giving it a *signature* of −1. Atoms linked by a line along which the density is a maximum with respect to any neighboring line, a bond path, are bonded to one another and share a common interatomic surface.[4] Thus the hydrogen is bonded to both the Si and Mn atoms in the adduct. It is important

(1) Lichtenberger, D. L. *Organometallics* **2003**, *22*, 1599−1602.
(2) Nikonov, G. I. *Organometallics* **2003**, *22*, 1597.
(3) Bader, R. F. W. *Atoms in molecules: a quantum theory*; Oxford University Press: Oxford UK, 1990.
(4) Bader, R. F. W. *J. Phys. Chem. A* **1998**, *102*, 7314−7323.

10.1021/om049450g CCC: $27.50
Publication on Web 11/12/2004

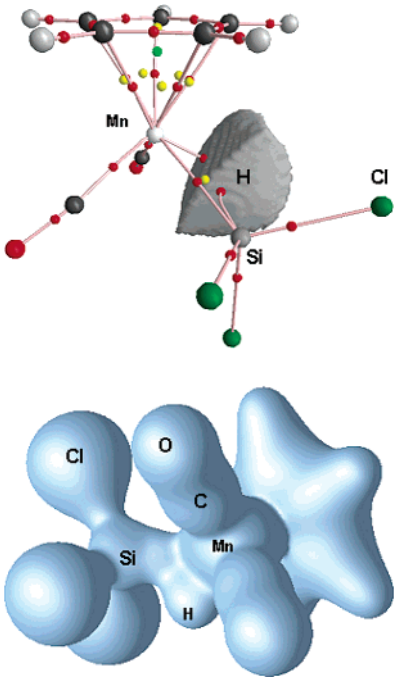

Figure 1. Upper diagram is the molecular graph of the adduct (CPs denoted by dots, nuclei by spheres) together with the two interatomic surfaces that separate the basin of the hydridic hydrogen from the basins of the Mn and Si atoms, the Si being bonded to three chlorines whose nuclei are denoted by green spheres. The Mn is linked by a bond path to each of the Cp carbons (black) and to the two carbonyl carbons, as well as Si and H. Bond CPs are denoted by red dots, ring CPs by yellow dots, and the single cage CP by a green dot. Note the close proximity of the ring CP of the three-membered |Mn|Si|H| ring to the Mn−Si bond CP. A stable CP is characterized by its three principal curvatures giving it a *rank* of 3. Since the density is a maximum at the bond CP in an interatomic surface, the two principal curvatures of the density at the CP are negative. The associated curvature along the bond path is positive, since the density is a minimum at the CP along this line. Thus two of the principal curvatures of a bond CP are negative and one is positive. The sum of their algebraic signs determines the *signature* of the CP, equal to −1, and a bond Cp is designated (3,−1). Since the two curvatures in the surface of a ring at a ring CP are positive (the density in the ring surface is a minimum at the ring Cp), while that along the ring axis negative, its designation is (3,+1). Lower diagram is an envelope map of the density set at the average value of $\rho_b = 0.072$ au, for the Mn−C links to the Cp ring to illustrate the bonded cone of density linking the Mn to the ring carbons. This is the lowest of the ρ_b values, and thus all pairs of enveloped atoms are bonded to one another, the bonding of the three-membered ring of Si, Mn, and H atoms being clearly displayed.

to appreciate that the identification of an atom in a molecule as an open quantum system and the criterion for bonding are inseparable, both being physical consequences of the topology of the density displayed at a (3,−1) or bond CP, a ubiquitous feature of charge distributions.

A *molecular graph*, the linked network of bond paths, defines a system's molecular structure, and is illustrated in Figure 1 for the adduct. The Mn is bonded to each of the carbon atoms of the Cp ring, to the carbons of the two carbonyl groups, and to the Si and hydridic hydrogen atoms. A molecular graph has been shown to recover the chemical structures in a multitude of systems, in terms of densities obtained from both theory and experiment. The chemical structures were previously inferred from classical models of bonding in conjunction with observed physical and chemical properties. There is always agreement between an accepted classical structure and the molecular graph, even in the case of electron-deficient molecules such as the boranes, which, as a result of spectroscopic observations, required the extension of the classical model to include bridging hydrogens and two-electron three-center bonding.[5] There are of course, many examples where classical models of bonding are inadequate to assign a structure and experimental evidence such as NMR couplings and spectroscopy are equivocal, as evidenced by the adduct considered here. The Mn, Si, and H atoms are seen to form a three-membered ring (3-MR), corresponding to the "valence bond structure" **3** (with the dotted line replaced by a bond path). The bonding determined by the molecular graph for the adduct and its energy of formation are the subjects of this paper.

The ability to assign a molecular structure based on information contained in the electron density obtained from either experiment or theory changes one's mode of attack. One now uses the structure defined by the molecular graph to rationalize and understand the experimental findings, rather than the reverse. This raises a most important point: since a molecular graph is the result of the forces that determine the observed properties of the molecule, it will always be in agreement with physical observation (assuming the availability of an adequate representation of the density). Those who doubt the universal identification of a bond path with bonding, citing the presence of bond paths between anions in an ionic crystal for example, should differentiate between classical models of bonding and its proper quantum mechanical description.[6]

The physical presence of bonding signifies an accompanying energetic stabilization, as every bond path is mirrored by a *virial path*, a line linking the same nuclei along which the electronic potential energy density is maximally stabilizing. Thus coexisting with every molecular graph is a shadow graph—the virial graph—indicating the presence of a corresponding set of lines, again defined in real space, that delineates the lowering in energy associated with the formation of the structure defined by the molecular graph.[7] Thus for example, the electron density of the anions in a crystal is diffuse and its condensation into bond paths linking the anions leads to a local lowering in the energy of the

(5) Longuet-Higgins, H. C.; Bell, R. P. *J. Chem. Soc.* **1943**, 250.

(6) The description of an ionic crystal as one whose cohesive energy is determined by electrostatic forces between the ions together with short-range core repulsions is a classical model without foundation in quantum mechanics. Matter is a distribution of charge in real space—of pointlike nuclei embedded in the diffuse density of electronic charge, $\rho(\mathbf{r})$, defined as the expectation value of the density operator.[20] The properties of $\rho(\mathbf{r})$ are determined by the local statements of the theorems of quantum mechanics, the most important being the Ehrenfest force theorem, determining its equation of motion, and the virial theorem, governing its energy. There is nothing in the quantum description of the energy corresponding to the classical model of interacting ions. In particular there are no resultant Ehrenfest forces acting on the atoms and no net forces, neither attractive nor repulsive, acting on the atomic nuclei, since the Feynman forces are zero and any displacement of a nucleus results in the creation of a force restoring it and its associated density to its equilibrium position.

(7) Keith, T. A.; Bader, R. F. W.; Aray, Y. *Int. J. Quantum Chem.* **1996**, *57*, 183−198.

crystal, as evidenced by the parallel condensation of the virial field into virial paths. The molecular graph for the adduct shown in Figure 1 is mirrored by its isomorphic virial graph.

Computations

Geometries were optimized using the 6-31+G* basis set in a calculation using the B3LYP DFT procedure given in GAUSSIAN98[8] and gave bond lengths reported in Å that are equal to or in better agreement with experiment than those reported by Lichtenberger for the adduct: Si−H, 1.795; Si−Mn, 2.326; and Mn−H, 1.554. The wave function for the minimum energy structure was redetermined using a large basis set for the atoms of primary interest and smaller sets for the remaining atoms: 6-311++G(2d,2p) for the atoms forming the three-membered ring (3-MR), Si, Mn, and H; 6-31+G* for the carbonyl and Cp carbons; 6-31G* for the Cl and O atoms; 3-21G* for the H atoms of the Cp ring. Corresponding basis sets were used to calculate the minimum energy geometries and structures for the reactants Cl_3SiH and $CpMn(CO)_2$, as well as for the closed-shell molecules $CpMn(CO)_3$ and $Mn(CO)_6^+$. The bond and atomic properties were calculated using AIMPAC[9] and AIM2000,[10] the latter program also being used in the construction of the diagrams. The delocalization indices are obtained using AIMDELOC.[11]

Electron Exchange and Electron Delocalization/Localization

The concepts of localization and delocalization of electrons play essential roles in chemistry. These concepts transcend orbital models, being instead consequences of the exclusion principle as embodied in the pair density. The role of the pair density is best made evident in the properties of the conditional same-spin density obtained by dividing the α-spin pair density $\rho^{\alpha\alpha}(\mathbf{r}_1,\mathbf{r}_2)$ by the spin density $\rho^{\alpha}(\mathbf{r}_1)$ (a similar expression holding for the β electrons), eq 1.

$$\rho^{\alpha\alpha}(\mathbf{r}_1,\mathbf{r}_2)/\rho^{\alpha}(\mathbf{r}_1) = \delta^{\alpha\alpha}(\mathbf{r}_1,\mathbf{r}_2) = [\rho^{\alpha}(\mathbf{r}_2) + h^{\alpha\alpha}(\mathbf{r}_1,\mathbf{r}_2)] \quad (1)$$

The conditional same-spin density $\delta^{\alpha\alpha}(\mathbf{r}_1,\mathbf{r}_2)$ determines the extent to which the exclusion principle decreases the density of an α electron at some position $\mathbf{r}_2$ when another α electron is assigned the position $\mathbf{r}_1$. [It must be understood that neither electron is fixed at either of these points, the charge of each being spread out in space in the manner determined by the spin density $\rho^{\alpha}(\mathbf{r})$.] The quantity $h^{\alpha\alpha}(\mathbf{r}_1,\mathbf{r}_2)$ describes the density of the Fermi hole. It equals the exchange density for α-spin electrons divided by $\rho^{\alpha}(\mathbf{r}_1)$. It is a negative quantity that describes the extent to which the density of the second electron is excluded from the neighborhood of $\mathbf{r}_1$. The integral of $h^{\alpha\alpha}(\mathbf{r}_1,\mathbf{r}_2)$ over $\mathbf{r}_2$ equals −1, corresponding to the removal of one α-spin electron. The exclusion is locally complete for $\mathbf{r}_1 = \mathbf{r}_2$, since $h^{\alpha\alpha}(\mathbf{r}_1,\mathbf{r}_1) = -\rho^{\alpha}(\mathbf{r}_1)$.[12] If $h^{\alpha\alpha}(\mathbf{r}_1,\mathbf{r}_2) \approx -\rho^{\alpha}(\mathbf{r}_2)$ for positions removed from $\mathbf{r}_1$, that is, the density of the Fermi hole is *localized* about this point, then all other α-spin electrons will be excluded from the space corresponding to the exclusion of one electronic charge. In a closed-shell system, the Fermi hole density of an electron of β-spin will be similarly localized, resulting in a pair of electrons being localized about the point $\mathbf{r}_1$. If on the other hand the density of the Fermi hole is diffuse, then the exclusion of same-spin electrons occurs over an extended region of space and the electron is *delocalized*.[13] The localization of the density of the Fermi hole to one atom is obtained by the double integration of the product $\rho^{\alpha}(\mathbf{r}_1)\ h^{\alpha\alpha}(\mathbf{r}_1,\mathbf{r}_2)$, the exchange density, over its basin yielding λ(A), the localization index for atom A. Its delocalization over two atoms, A and B, is obtained by a corresponding integration of the exchange density over both atomic basins to yield δ(A,B), the delocalization index.[14] One has the simple understanding that if the exchange of electrons is largely confined to within a given atomic basin, then the electrons are correspondingly localized on that atom, while if the electrons exchange between atomic basins, then the electrons are delocalized over both atoms or, equivalently, are shared by both atoms. Electrons that exchange are indistinguishable, and consequently, *the physical picture underlying electron delocalization is exceedingly simple—it is determined by the extent to which the electrons on one atom exchange with those on another.* Collectively, λ(A) and δ(A,B) are termed the exchange indices.

The delocalization index δ(A,B) is of particular importance in bridging classical notions of bonding and quantum mechanics. It provides a determination of the number of α,β electron pairs that are exchanged between two atomic basins, thus providing a physical measure of a property that classical models of bonding associate with covalency. The role of exchange in determining the energy is to reduce the electron−electron Coulomb repulsion between a pair of bonded atoms, and δ(A,B) counts the number of pairs contributing to this reduction, the "spin exchange resonance" of valence bond theory. The delocalization index provides a clear indication of the progression of bonding from "covalent" to "polar" to "ionic", an increasing localization of the electrons within the atomic basins that parallels increasing interatomic charge transfer, causing a reduction in δ(A,B). In the 14-electron molecules N_2 and CO, three electrons are exchanged between the atoms in homopolar N_2 (giving a Lewis bond order of 3) compared to only 1.6 in polar CO. In the12-electron molecules C_2 and LiF, the latter with atomic charges of ±0.93, δ(C,C) = 2.7, whereas δ(Li,F) = 0.19, the ionic limit being characterized by an almost total localization of the

(8) Frisch, M. J.; Trucks, G. W.; Schlegel, H. B.; Scuseria, G. E.; Robb, M. A.; Cheeseman, J. R.; Zakrzewski, V. G.; Montgomery, J. A., Jr.; Stratmann, R. E.; Burant, J. C.; Dapprich, S.; Millam, J. M.; Daniels, A. D.; Kudin, K. N.; Strain, M. C.; Farkas, O.; Tomasi, J.; Barone, V.; Cossi, M.; Cammi, R.; Mennucci, B.; Pomelli, C.; Adamo, C.; Clifford, S.; Ochterski, J.; Petersson, G. A.; Ayala, P. Y.; Cui, Q.; Morokuma, K.; Malick, D. K.; Rabuck, A. D.; Raghavachari, K.; Foresman, J. B.; Cioslowski, J.; Ortiz, J. V.; Stefanov, B. B.; Liu, G.; Liashenko, A.; Piskorz, P.; Komaromi, I.; Gomperts, R.; Martin, R. L.; Fox, D. J.; Keith, T.; Al-Laham, M. A.; Peng, C. Y.; Nanayakkara, A.; Gonzalez, C.; Challacombe, M.; Gill, P. M. W.; Johnson, B. G.; Chen, W.; Wong, M. W.; Andres, J. L.; Head-Gordon, M.; Replogle, E. S.; Pople, J. A. *Gaussian 98*, revision *A.9*; Gaussian, Inc.: Pittsburgh, PA, 1998.

(9) Biegler-König, F. W.; Bader, R. F. W.; Tang, T.-H. *J. Comput. Chem.* **1982**, *13*, 317−328. AIMPAC can be downloaded from (http://www.chemistry.mcmaster.ca/aimpac/).

(10) Biegler-König, F.; Schönbohm, J. *J. Comput. Chem.* **2002**, *23*, 1489−1494.

(11) Matta, C. F. AIMDELOC (QCPE0802). *Quantum Chemistry Program Exchange,* Indiana University (http://qcpe.chem.indiana.edu/), 2001.

(12) Mcweeny, R. *Rev. Mod. Phys.* **1960**, *32*, 335.

(13) Bader, R. F. W.; Stephens, M. E. *J. Am. Chem. Soc.* **1975**, *97*, 7391−7399.

(14) Fradera, X.; Austen, M. A.; Bader, R. F. W. *J. Phys. Chem. A* **1999**, *103*, 304−314.

electrons within the basins of the individual atoms with a minimal exchange between them. Pendas et al.[15] have recently constructed a program enabling the determination of the atomic contributions to the exchange energy. As anticipated, one finds the interbasin exchange energies V_{ex}(A,B) to parallel the relative values of the delocalization indices. In a private communication, Pendas finds V_{ex}(N,N) = −0.951 au and V_{ex}(C,O) = −0.442 au, giving a ratio of 2, identical to the ratio of the delocalization indices for the 14-electron series. In the 12-electron series, V_{ex}(C,C) = −0.717 au compared to V_{ex}(Li,F) = −0.045 au, giving a ratio of 16 compared to a value of 15 for the delocalization indices. The contribution of the "α,β spin exchange resonance" resulting from exchange of electrons between atomic basins clearly decreases with increasing polarity of the interaction, its value in ionic LiF accounting for only 0.4% of the total exchange energy, the remainder being localized within the individual atomic basins.

The limiting value of the atomic localization index λ(A) is N(A), the population of A, corresponding to the complete localization of the electrons on A. Since electron exchange corrects for the self-repulsion of the electrons, N in number, the summation of the indices λ(A) and δ(A,B) over all atoms in a molecule, yields N. The exchange indices thus account for all of the electrons, determining the number localized on each atom and the number delocalized, that is, shared or exchanged, between every pair of atoms. The delocalization indices for bonded atoms at the Hartree−Fock level may be interpreted as bond orders in relation to the Lewis electron pair model.[14] The equal sharing of a pair of electrons between A and B requires that the density equivalent to one electron be shared between them, giving δ(A,B) = 1, and that the density equivalent to a second electron be equally localized within the basins of A and B, giving λ(A) + λ(B) = 1. Thus one, two, or three pairs of electrons equally shared between two atoms yield delocalization indices of 1, 2, or 3, respectively. The values of δ(C−C) = 1.26 and δ(C−H) = 0.92 for the Cp ring, Table 1, are the anticipated bond orders for a C−C aromatic and C−H bonding. Significant charge transfer between the bonded atoms increases the degree of localization within each atomic basin, the values of λ(A) and λ(B), and hence reduces the value of δ(A,B).

Bonding in the Adduct

Table 1 lists the values of δ(A,B) for bonded atoms and values of selected properties at the bond CP for the adduct and the changes from the reactant values for Si−H: the value of the density ρ_b, the energy density H_b determined by the local statement of the virial theorem, and the ellipticity ϵ, determining the extent to which the density is accumulated in a given plane. Table 1 lists averaged values for the chemically equivalent Mn−C, C−C, C−H, and Si−Cl interactions. The indices for the C−C and C−H bonding in a Cp ring are typical of shared interactions; ρ_b > 0.25 au, and negative values for the energy density H_b. A value of ϵ > 0 signifies the presence of "π" density, and the value of 0.21 for the C−C bond paths in the Cp ring is typical of an aromatic system (ϵ = 0.23 for benzene), with the diffuse density accumulated on either side of the ring plane. A significant bond ellipticity, ϵ > 1, indicates that the bond path is susceptible to rupture by a suitable change in geometry, a feature utilized in the discussion of the stability of the adduct.

Table 1. Delocalization and Bond Indices for Adduct in au

A−B	δ(A,B)	ρ_b	H_b	ϵ
Mn−H	0.650	0.117	−0.053	0.158
Mn−Si	0.575	0.080	−0.032	1.079
Si−H	0.311	0.083	−0.034	0.722
(reactant)	0.571	0.134	−0.101	0.000
Mn−C(O)	1.086	0.145	−0.063	0.130
Mn−C(Cp)	0.369	0.072	−0.046	3.117
C−O	1.518	0.457	−0.770	0.002
C−C	1.258	0.294	−0.279	0.210
C−H	0.922	0.277	−0.233	0.013
Si−Cl	0.560	0.092	−0.054	0.038

Table 2. Atomic and Group Charges in Adduct and Changes in ΔN(A) and ΔE(A) from Reactants

A	q(A), e	ΔN(A), e	ΔE(A), kcal/mol
Mn	+0.817	+0.125	+62
Si	+2.091	+0.572	−119
H	−0.284	−0.330	+73
Cl	−0.695	+0.012	−26
Cp	−0.133	−0.193	+1.1
CO	−0.201	−0.105	+18
SiCl3	+0.006	+0.609	−197

The small values of ρ_b for the bonded interactions with Mn are typical of bonding to a transition metal atom M. The values of ρ_b for bonding to a carbonyl carbon fall within 0.11−0.14 au, the range of values found for the carbonyl complexes of Cr, Fe, and Ni.[16] What is also typical of M−C bonding in the carbonyl complexes is the almost equal sharing of one electron pair between M and C, the values of δ(M,C) ranging from 0.8 to 1.0 in the carbonyl complexes compared to the values of 1.1 to 1.2 found in $CpMn(CO)_2$, $CpMn(CO)_3$, and the adduct. Bonding to M is also characterized by negative values, small in magnitude, for the energy density H_b. The small values of ρ_b and $|H_b|$ are a result of the bond CP for M−L falling in the outer shell of charge depletion of the metal atom, the region where $\nabla^2\rho(\mathbf{r}) > 0$.[17] The nearly equal sharing of one Lewis pair in the M−L interactions is indicative of a shared interaction, one that in the case of the metal carbonyls yields an average M−C bond energy in the range 26−35 kcal/mol.[16]

The Mn−H and Mn−Si interactions in the 3-MR formed from the Mn, Si, and H atoms also exhibit significant delocalization indices, 0.7 and 0.6, respectively, despite their extended separations. The smallest bond order in the 3-MR is between Si and H. This is an understandable result, as the bonding is between atoms bearing substantial net charges of +2 and −0.3, Table 2, and the value of 0.3 for δ(Si,H) indicates a degree of exchange characteristic of a polar interaction. A comparison of the δ(Si,H) and bond CP values for the adduct with those for the reactant $HSiCl_3$, Table 1, provides a measure of the weakening of the Si−H bonding in

(15) Pendás, A. M.; Francisco, E.; Blanco, M. A. *J. Chem. Phys.* **2004**, *120*, 4581.

(16) Cortés-Guzmán, F.; Bader, R. F. W. *Coord. Chem. Rev.* **2004**, in press.

(17) Gervasio, G.; Bianchi, R.; Marabello, D. *Chem. Phys. Lett.* **2004**, *387*, 481−484.

forming the adduct. The value of ρ_b and the magnitude of H_b decrease, by 38 and 66%, respectively, while δ(Si,H) decreases by 46%. The latter decrease is in line with the decrease in the J(Si−H) coupling constant observed in the formation of the adduct, a proton coupling constant being dominated by the Fermi contact term that is proportional to the integral of the exchange density over the H basin.[18] Lichtenberger estimates an 80% weakening in the Si−H bonding in the adduct based on a comparison of the J(Si−H) values in the adduct with those in $HSiCl_3$ and $(CO)_4Fe(H)SiCl_3$. The present results are consistent with and complement Lichtenberger's description of the reaction as one leading to the formation of the Mn−H interaction at the expense of a weakening in the Si−H interaction, the opposite view of that expressed by Nikonov.[2]

Table 2 lists the charges on each atom, q(A). An atomic population is the measurable expectation value of a Dirac observable[19,20] and is routinely measured in accurate X-ray diffraction experiments. The advent of synchrotron radiation sources and CCD detectors has greatly enhanced the accuracy of the experimentally determined density and enabled charge-density studies on molecules of ever-increasing size. The agreement between experiment and theory in the determination of atomic properties and bond indices is similar to the agreement between different theoretical calculations.[21] The charge on manganese, $q(Mn) = +0.82$, is typical of charges on metal atoms in complexes with Cp and CO ligands. It is intermediate between the charges on neighboring periodic atoms in their carbonyl complexes, with $q(Cr) = +1.2$, $q(Fe) = +0.74$, and similar to the charges on the metals in metallocenes for which $q(Fe) = +0.79$ and $q(Ge) = +0.87$.[16] The diagonal elements of the atomic overlap matrix, composed of the overlaps of MOs over each atomic basin, demonstrate that the 18-electron cores in all of these molecules are essentially completely localized on the metal atoms, undergoing minimal exchange with the "valence density", the latter defined to be the remainder of the population on the metal. Thus Mn has a well-defined valence population of 6.2e, implying the presence of six d electrons in the orbital model of electronic structure.

When gauged relative to a neutral Mn atom, the electronic charge transferred to each of the ligand atoms is relatively small: 0.13e to the Cp ring, 0.20e to each CO group, 0.28e to the bonded hydrogen atom imparting hydridic character. While the Si atom bears a charge of +2e, this is a result of the charge transfer to the Cl atoms, the charge on the $SiCl_3$ group being only +0.01e. With six valence electrons and moderate charge transfer to the ligands, one anticipates the bonding of the Mn to the ligands will be typical of shared interactions, as reflected in the bond and delocalization indices.

The difference between the population of Mn, $N(Mn) = 24.2$, and the number of electrons localized within its basin, $\lambda(Mn) = 21.2$, demonstrates that three of the six Mn valence electrons are delocalized over the ligands. Since the ligands exchange an equal number of electrons, there are a total of six electrons delocalized between Mn and the ligands. Of these, 0.7e is exchanged with the hydridic hydrogen, 0.6e with the Si, another 2.2e are exchanged with the carbonyl carbons, and 1.9e with the carbons of the Cp ring. The remaining 0.8e is delocalized over the remaining atoms, those not bonded directly to Mn. The 1.9 electrons exchanged between Mn and the carbons of the Cp ring translates into the sharing of approximately two Lewis pairs, a value that is unchanged from that found in the reactant $CpMn(CO)_2$. These values are in agreement with Moffit's pioneering molecular orbital study of the bonding in $FeCp_2$, wherein he argued that the bonding of a Cp ring to the iron atom depicted by five "bonds" is a result of the participation of two Lewis pairs.[22] The value of δ(Fe,C) in ferrocene is found to be 0.328e, corresponding to the sharing of 1.6 Lewis pairs of Fe with a Cp ring, a value somewhat less than the number shared by Mn with Cp in the adduct.[16]

The interaction of Mn with the carbons of the Cp ring depicted by five bond paths in the molecular graph requires comment. The chemical structures of a metal atom M bonded to an unsaturated ring are sometimes denoted by "bonds" linking M to each carbon of the ring and at other times by a single "bond" linking the metal atom to the center of the unsaturated ring. The cyclopentadienyl complexes are electron-deficient molecules in the Lewis sense, in agreement with Moffit's argument that the interaction of Fe with a Cp ring in ferrocene depicted by five "bonds" is the result of the sharing of two electron pairs. The linking of the metal atoms to carbons of the Cp rings results in the formation of five 3-MRs and a (3,+1) or ring CP is present in the face of each ring, the point where the density attains its minimum value in the ring surface, Figure 1. There is a ring CP in the center of the Cp ring as well, and this ring surface, together with the five surfaces formed by the links to the metal atom, defines a cage enclosing a (3,+3) or cage CP. Each ring CP of a 3-MR lies on a line linking the neighboring bond CPs, Figure 1, and it has a value, ρ_r, that is only 0.002 au less than ρ_b, the lowest value of the density present in the perimeter of each ring. The result is a ring of alternating bond and ring CPs girdling the cage that is of almost constant density, with a value of 0.072 ± 0.003 au. Thus the bonding of a metal atom to an unsaturated ring is not well represented in terms of a set of individual bond paths, but rather by a bonded cone of density, with the density at any point on an individual bond path having a value only slightly in excess of that for points displaced off the bond path into the faces of the neighboring rings. This feature of the metal−ring interaction is depicted in the display of a density envelope with the value 0.072 au, Figure 1. Clearly, the interaction of a metal atom with a Cp ring is best viewed as involving an interaction with the delocalized density of the entire ring perimeter, a picture that is conceptually similar to that used to denote the interaction of a metal with an unsaturated ring in a conventional chemical structure. As noted above, the delocalization indices indicate that approximately two pairs of electrons are shared between Mn and the Cp ring, and the result is an enhanced

(18) Matta, C. F.; Hernández-Trujillo, J.; Bader, R. F. W. *J. Phys. Chem. A* **2002**, *106*, 7369−7375.
(19) Bader, R. F. W.; Matta, C. F. *J. Phys. Chem A* **2004**, *108*, 8385−8394.
(20) Bader, R. F. W.; Zou, P. F. *Chem. Phys. Lett.* **1992**, *191*, 54−58.
(21) Scheins, S.; Dittrich, B.; Messerschmidt, M.; Paulmann, C.; Luger, P. *Acta Crystallogr.* **2004**, *B60*, 184−190.
(22) Moffitt, W. *J. Am. Chem. Soc.* **1954**, *76*, 3386.

binding over what one would anticipate on the basis of the individual ρ_b values. The delocalization of the bonding density over ring surfaces is characteristic of electron-deficient systems as found, for example, for the surfaces of 3- and 4-MRs formed by the boron and/or carbon atoms in boranes and carboranes.[23]This view of metallocene bonding was previously put forth in the description of the interaction of titanium with a Cp ring[24] and in the metallocenes of Al^+, Fe, and Ge,[16] a view consistent with the low barrier to rotation of the Cp ring in metallocenes.

Lichtenberger, after presenting arguments based on HOMO/LUMO in a frontier orbital model, states, "Of course any orbital description is an approximation of the electronic structure, but the electron distributions discussed above can be demonstrated by the total electron density." A density envelope of value equal to 0.08 is displayed and stated to show that "the Mn−hydride interaction is well formed in comparison to the other bonds in the molecules". Depending upon what value of the density is chosen, one may demonstrate any atomic connection. The envelope map of the density shown in Figure 1 is for the smallest of the ρ_b values, and thus all bonded pairs of atoms are linked by bridges in the density and atoms not so linked are not bonded. The qualitative information provided by this envelope, whose purpose was to demonstrate the bonded cone of density linking Mn to the Cp ring, is, of course, made quantitative by the molecular graph shown in Figure 1 and the ρ_b values given in Table 2. The reader may compare this information, obtained from the topological analysis of the density, with that conveyed by the density envelope displayed by Lichtenberger, his Figure 12.

Stability of Ring Structure

The Mn, Si, and H atoms form a 3-MR structure with the Mn−Si interaction exhibiting a significant ellipticity, $\epsilon = 1.1$. This is a consequence of its bond CP being in close proximity with the CP for the 3-MR, Figure 1, a harbinger of the possible rupture of the Mn−Si bond path. The topological theory of structure provides a description of all possible changes of a given structure into neighboring structures, each attained by particular nuclear motions.[25] The structure diagram for a 3-MR system composed of Si, H, and Mn atoms is illustrated schematically in Figure 2.[3] It shows the boundaries imposed on the space of nuclear configurations that partition the possible molecular geometries into different structural regions. The boundaries are the "catastrophe set", the set of geometries corresponding to unstable structures. In addition to yielding anticipated structures including the "σ-bond" complex, structure **1**, it excludes certain other structures, such as **6** given in Lichtengberg's paper, that have been proposed for the adduct.[2]

The ring structure is attained through the approach of the Mn atom to the Si−H bond path to give a structure wherein the Mn is bonded to the Si−H bond CP to yield a "conflict structure" corresponding to structure **1**. This structure in unstable and zero-point motions will result in the bond path from Mn terminating alternately at the Si and H nuclei to give the neighboring structure Mn−Si−H or Mn−H−Si. The closer approach of the Mn to H causes a lengthening of the Si−H separation, leading to the bifurcation of the bond CP linking the Mn to the Si−H bond path into two bond CPs and a ring CP, and the adduct enters the geometrical region associated with the ring structure. It is characterized by relatively long Si−H and Si−Mn separations, 1.8 and 2.3 Å, respectively, compared to the Mn−H separation of 1.5 Å. The Si−H bond path is inwardly curved, resulting in a bond path length that is significantly longer, by 0.12 Å, than the bond length, Figure 2.

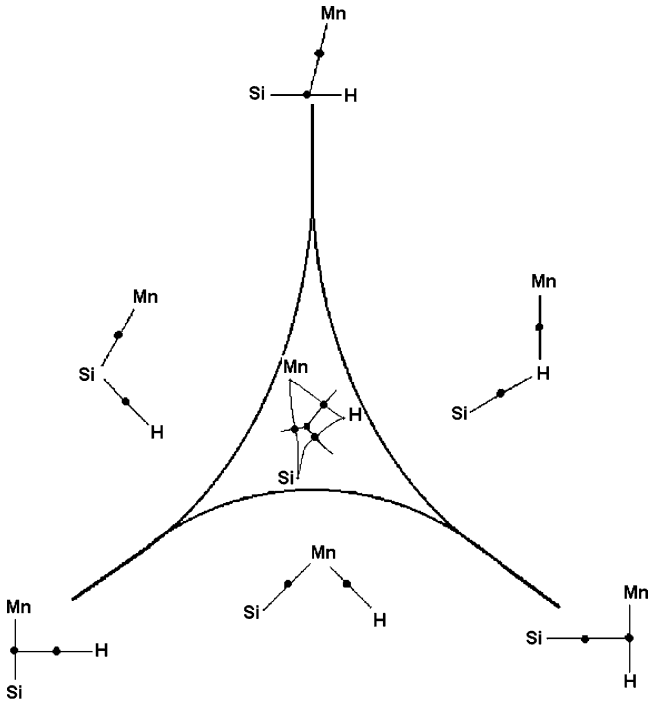

Figure 2. Schematic representation of the structure diagram for the three-atom Mn, Si, H system showing the ring structure and the three possible open structures. Neighboring open structures are separated by a line of unstable conflict structures, while the ring structural region is bounded by the set of unstable bifurcation structures obtained when the ring CP coalesces with one of the three bond CPs. The molecular graph of the |Mn|Si|H| ring for the equilibrium structure is inscribed within the ring region with the bond CPs denoted by dots. The interatomic surfaces of the ring atoms intersect at the position of the ring CP. Note the inwardly curved nature of the Si−H bond path and the close proximity of the ring CP to the CPs of the Si−Mn and Si−H bond CPs, a harbinger of the susceptibility to ring opening by rupture of either of these bond paths.

The opening of a ring structure occurs when the ring CP, the point of lowest density in the ring surface whose value is denoted by ρ_r, coalesces with a bond CP of the 3-MR, the point of lowest density along the bond path. The ring CP lies closest to the bond CP of Mn−Si, a distance of 0.24 Å, as indicated in Figure 2, and the structure is predicted to be most susceptible to change by the breaking of the Mn−Si bond path to yield the

(23) Bader, R. F. W.; Legare, D. A. *Can. J. Chem.* **1992**, *70*, 657−676.
(24) Bader, R. F. W.; Matta, C. F. *Inorg. Chem.* **2001**, *40*, 5603−5611.
(25) Bader, R. F. W.; Nguyen-Dang, T. T.; Tal, Y. *Rep. Prog. Phys.* **1981**, *44*, 893−948.

open structure Mn−H−Si. However, the density is relatively flat over the ring surface, with the values of the density at the bond CPs for Mn−Si and Si−H being in excess over ρ_r by only 0.01 and 0.04 au, respectively, and because of the inwardly curving nature of the Si−H bond path, the ring CP is also in close proximity to the bond CP of Si−H, with a separation of 0.34 Å. Thus the curvature of the density in the ring surface at the ring CP lying on the axis directed at the Mn−Si bond CP has a small positive value equal to 0.04 au, while the magnitudes of the curvatures of the Mn−Si and Si−H bond CPs lying in the plane and directed at the ring CP are equally small, 0.03 and 0.05 au, respectively. The density rises more steeply toward the Mn−H bond CP with $\rho_b = 0.12$ au, a distance 0.7 Å from the ring CP. Thus one anticipates that the ring structure will be susceptible to opening by rupture of either the Mn−Si or Si−H bond paths.

This prediction is in line with a vibrational analysis of the adduct that yields frequencies in cm^{-1} and force constants in mdyn/Å, the latter values in parentheses, of 292 (0.84), 919 (0.54), and 1929 (2.26), respectively, for the lowest frequency stretches of Si−Mn, Si−H, and Mn−H using the 6-31+G* basis. One notes that the order of the frequencies parallels that of the ρ_b values and is inversely related to the corresponding bond ellipticities. Both the topological and force constant analyses point to the Mn−Si and Si−H bond paths as the ones most susceptible to rupture.

Increasing the Si−Mn separation by 0.01 Å accompanied by a reoptimization of all remaining geometrical parameters results in an energy increase of only 0.09 kcal/mol and causes the Si−Mn bond and ring CPs to approach to within 0.16 au of one another, bringing their values to within 0.0002 au, with $\rho_b = 0.0787$ au. The ellipticity of the Si−Mn bond path increases to 2.6, and the bond and ring CPs are on the verge of coalescence. A further increase in the Si−Mn separation by 0.04 au that is accompanied by an increase of 0.16 kcal/mol in energy yields the open structure. Lichtenberger points out that the DFT calculations appear to overestimate the length of the Mn−Si bond compared to the experimental value of 2.254 Å obtained from an X-ray analysis of an analogue of the adduct with a methyl-substituted Cp ring.[26,27] It is thus of interest to also compare the effect of *decreasing* the Mn−Si separation to the experimental value in the crystal. The result obtained could be anticipated in view of the properties of the density in the ring surface where nuclear motions that effect changes in a "flat" density distribution are effected with little increase in energy. Thus decreasing the Mn−Si separation with reoptimization of the remaining parameters causes the energy to increase by only 0.6 kcal/mol and results in the migration of the ring CP toward the bond CP of the Si−H bond path, increasing its ellipticity to 1.05 and reducing the separation between the two CPs to 0.24 Å, the same properties associated with the Mn−Si CP in the equilibrium structure. Thus reducing the Mn−Si separation imparts instability to the Si−H bond, while increasing it destabilizes the Mn−Si bond. A DFT calculation does not fail in its prediction of a "short" Mn−Si bond length, the difference with experiment being the result of a very flat potential energy surface for relative motions of the Mn and Si nuclei with the attendant difficulty of finding an absolute minimum.

Clearly the ring structure survives only as the result of the averaging of the bond path that terminates at Si oscillating between the Mn and H atoms, the Mn−H interaction being structurally stable. It should not be assumed that the instabilities associated with the Si−Mn and Si−H bond paths imply any instability in the interaction of $|Si-Cl_3$ with the remainder of the system, the following analysis showing that the major charge transfer is from the $CpMn(CO)_2H|$ group to the $|SiCl_3$ group. Instead, because of the significant charge transfer, this interaction has little directional preference and is characterized by a facile switching of the terminus of the bond path to Si from the Mn atom to the H atom. These features of the potential energy surface have been brought to the fore by the coupling of the bond critical point analysis with the structure diagram.

Charge and Energy Changes in Formation of the Adduct

While the structure of the adduct corresponds to that anticipated from oxidative addition, with the formation of bond paths linking H and Si to Mn, the interatomic charge transfers incurred during the reaction do not correspond to those anticipated on the basis of a formal electron count.[28] (Table 2 includes the changes in the atomic populations relative to their values in the reactants.) The largest change incurred in the formation of the adduct is the transfer of 0.57e to Si, with another 0.04e being transferred to the Cl atoms. The flow of density to the $SiCl_3$ group reduces its charge from +0.62e in the reactant to −0.01e in the adduct. The value of q(Mn) undergoes a slight reduction, the population of Mn increasing by 0.125e. The principal source of the electrons is the hydridic hydrogen, the lengthening and weakening of the Si−H bonding, and the concomitant bonding of H to Mn, resulting in a loss of 0.33e. There is a further transfer of 0.21e from the CO groups (80% from C) and 0.19e from Cp.

The calculated change in energy, ΔE, for the formation of the adduct is −24.9 kcal/mol. The largest stabilizing contribution to ΔE of −197 kcal/mol comes from the $SiCl_3$ group, the Si atom contributing −119 kcal/mol. The remaining atoms and groups are all destabilized, Mn by 62 kcal/mol, the hydridic H by 73 kcal/mol, the CO groups by 36 kcal/mol, and the Cp group by 1 kcal/mol. In summary, the oxidative addition character of the reaction is the result of the transfer of 0.61e to the $SiCl_3$ group, 0.28e from the $(CO)_2MnCp$ group and 0.33e from the hydridic hydrogen, with the proviso that Mn undergoes a slight reduction in the process.

Laplacian Distribution and Electron Localization

Lichtenberger points out that the description of the frontier orbitals of the $CpMn(CO)_2$ adduct developed by

(26) Schubert, U.; Ackmermann, K.; Kraft, G.; Woerle, B. *Naturforsch.* **1983**, *38B*, 1488.
(27) Schubert, U. *Adv. Organomet. Chem.* **1990**, *30*, 151.
(28) Collman, J. P.; Hegedus, L. S.; Norton, J. R.; Finke, R. G. *Principles and Applications of Organotransition Metal Chemistry*; University Science Books: Mill Valley, CA, 1987.

Hoffmann et al. from molecular orbital models has had wide success in explaining the chemistry of this group.[29] They obtained the fragment orbitals for $CpMn(CO)_2$ from related systems, finding a three below two splitting of the d block, typical of a pseudo-octahedron, with the degeneracies further lifted within each set. The set of three, whose uppermost member is the HOMO together with the LUMO, the lowest member of the 2-fold set, comprise the four "crucial orbitals". He uses the resulting frontier orbital arguments to account for the formation of the adduct, focusing in particular on the potential "π" donating ability of the HOMO with the approaching ligand and on the acceptor properties of the LUMO, which has minimal interaction with the Cp^- and CO ligands. This section is devoted to demonstrating that the understanding and predictions obtained from the frontier orbital model are faithfully recovered in the properties of the Laplacian of the electron density, a distribution whose properties are determined by the properties of the electron pair density.

The localization of electrons is of equal importance to their delocalization, underlying the concept of Lewis electron pairs. The Laplacian of the density determines where density is locally *concentrated*, where $\nabla^2\rho(\mathbf{r}) < 0$, and locally *depleted*, where $\nabla^2\rho(\mathbf{r}) > 0$. Since $\nabla^2\rho(\mathbf{r}) < 0$ denotes a concentration of density, one defines the function $L(\mathbf{r}) = -\nabla^2\rho(\mathbf{r})$, a maximum in $L(\mathbf{r})$ denoting a maximum in the concentration of the density, a local charge concentration or CC. The topology of $L(\mathbf{r})$ provides a link between models of localized electrons and a measurable property of the electron density,[30] a link originally surmised because of the faithful mapping of its local charge concentrations onto the number, relative size, and angular orientation of the bonded and nonbonded electron pair domains assumed in Lewis electron pair theory and the VSEPR model of molecular geometry.[31] This empirical link has since received theoretical justification.[32] In the instance of the Fermi hole being strongly localized about $\mathbf{r}_1$, the conditional same-spin density, eq 1, will approach the single-particle spin density in regions $\mathbf{r}_2$ removed from the region of localization. In such regions, the sum of the α and β conditional pair densities will approach the total density $\rho(\mathbf{r}_2)$ for a closed-shell system, and consequently, the Laplacian of the conditional pair density will approach $L(\mathbf{r})$. Thus the topology of the Laplacian of the conditional pair density exhibits a homeomorphism with the topology of $L(\mathbf{r})$, one that approaches an isomorphic mapping of one field onto the other. As a consequence of this mapping, the CCs displayed in $L(\mathbf{r})$ signify the presence of *regions of partial pair condensation, that is, of regions with greater than average probabilities of occupation by a single pair of electrons*. It is important to understand that the concept of "partial pair condensation" does not imply the association of a single pair of electrons with each CC, but rather, that the associated decrease in the average pair population imbues the region with the properties associated with the bonded and nonbonded "electron pairs" of chemistry. The degree of sharing and localization of the electrons is determined by the exchange indices.

Bonded interactions result in the formation of CCs on the surface of the outermost shell of charge concentration of an atom, termed its valence shell charge concentration (VSCC). Since the integral of $L(\mathbf{r})$ over an atom integrates to zero, the creation of local concentrations of charge within the VSCC of an atom must also result in the creation of regions of charge depletion. *It is the complementary mapping of the maxima or "lumps" with the minima or "holes" between the reactant molecules that defines Lewis acid−base reactions.* Such Lewis complementarity is the density embodiment of the "lock and key" analogy proposed by Ehrlich to account for the high degree of antibody specificity, an idea that resulted in his introduction of the term "receptor" into the language of physiological chemistry.[33] Applications of Lewis complementarity to biological systems have been summarized,[34] and MacDougall and Henze give a number of displays of the reactive surfaces determined by Laplacian envelopes of biological molecules, identifying in particular the key reactive sites in penamecillin.[35] Lewis complementarity determines the dynamic and static aspects of the donor−acceptor interactions of transition metal complexes with incomplete d shells.

The structure of an atomic Laplacian is summarized by its atomic graph, the polyhedron whose vertexes (V) are defined by the CCs present in its VSCC. The edges (E) connecting the CCs of the polyhedron are defined by the unique pairs of trajectories originating at the intervening (3,−1) CPs. Each of the resulting faces (F) contains a (3,+1) CP. The vertexes denote the maxima in *charge concentration*; the faces denote the regions of *charge depletion* in the VSCC. The atomic graph is classified by its characteristic set [V,E,F], giving the number of each type of CP and satisfying Euler's relation $V - E + F = 2$. For first-row transition metal atoms the atomic graph describes the structure present in the third quantum shell. The characteristic set of a transition metal atom M determines its donor−acceptor characteristics, as embodied in the association of a charge concentration (CC) on one reactant with a charge depletion (CD) on another. The association CC ↔ CD provides a physical complement to models based on frontier orbital arguments.

The atomic graph maps onto the crystal and ligand-field descriptions of the electronic structure of M. The atomic graph of an octahedral or near octahedral d^6 complex has a cubical structure with the characteristic set [8,12,6], as exemplified by the polyhedron for Mn in $Mn(CO)_6^+$ displayed in Figure 3. This atomic graph is the homoeomorphic image of that for Cr in $Cr(CO)_6$, another d^6 system.[16] The topological features associated with the CCs and CDs of an atomic graph are best displayed in the form of an envelope map for $L(\mathbf{r})$, one that clearly defines the "lumps" and "holes", Figure 3. The location of the maxima and minima in an atomic

(29) Schilling, B. E. R.; Hoffmann, R.; Lichtenberger, D. L. *J. Am. Chem. Soc.* **1979**, *101*, 585−591.
(30) Bader, R. F. W.; MacDougall, P. J.; Lau, C. D. H. *J. Am. Chem. Soc.* **1984**, *106*, 1594−1605.
(31) Gillespie, R. J.; Hargittai, I. *The VSEPR Model of Molecular Geometry*; Allyn and Bacon: Boston, MA, 1991.
(32) Bader, R. F. W.; Heard, G. L. *J. Chem. Phys.* **1999**, *111*, 8789−8798.
(33) Ehrlich, P. *Lancet* **1913**, *2*, 445.
(34) Bader, R. F. W.; Matta, C. F.; Martin, F. J. *Quantum Medicinal Chemsitry*; Carloni, Alber, F., Eds.; Wiley-VCH: Weinheim, Germany, 2003.
(35) MacDougall, P. J.; Henze, C. E. *Theor. Chim. Acc.* **2001**, *105*, 345−353.

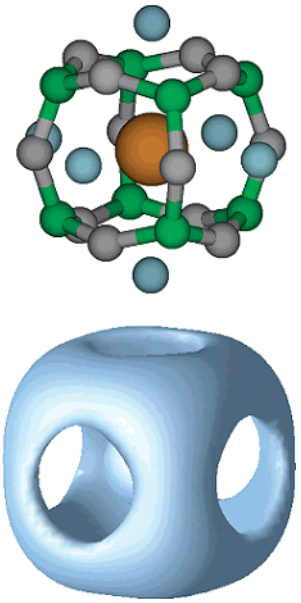

Figure 3. Stick representation of the atomic graph for the Mn atom in $Mn(CO)_6^+$ above a display of its envelope. Each green sphere represents a vertex in the atomic graph, a CC or (3,−3) CP in $L(\mathbf{r})$. The CCs are linked to one another by lines emanating from intervening (3,−1) CPs that form the edges of the atomic graph. Each face contains a (3,+1) CP denoted by a blue sphere, a point of minimum charge concentration in the surface of the atomic graph. The inner sphere is the inner core of charge concentration. The envelope map, for $L(\mathbf{r}) = 17$ au, demonstrates the 12 regions of charge concentration and the six regions of charge depletion that assume the roles of the t_{2g} and e_g orbitals of crystal or ligand field theory in the Laplacian description of donor−acceptor interactions.

graph for a d^6 complex coincides with the pattern predicted by crystal field theory, with the vertexes or CCs corresponding to the occupied t_{2g} set and the faces or CDs, the regions of charge depletion, corresponding to the empty e_g set, a feature first pointed out by Bo et al.[36,37] Macchi and Sironi[38] have drawn attention to the similarity exhibited by density of the $(t_{2g})^6$ set of electrons with the envelope representation of $L(\mathbf{r})$. Ligand field theory distinguishes between the t_{2g} and e_g orbitals through their differing overlaps with the ligand orbitals, the former with π, the latter with σ, and it yields a modified interpretation of the atomic graph. The eight CCs in the atomic graph are associated with the t_{2g} orbitals that overlap with the π orbitals of the ligands, while the six faces or centers of charge depletion are associated with the e_g set that participate in σ bonding with the ligands. It is shown below that the CCs are associated with the transfer of density from M to the π^* orbitals of the ligands in accord with the Chatt−Duncanson $d\pi-p\pi^*$ back-bonding model.[39] The association of the holes in the atomic graph with the σ bonding to the metal is in accord with the small transfer of charge from the ligand σ orbitals to the metal determined by the analysis of the orbital contributions

(36) Bo, C.; Poblet, J. M.; Bénard, M. *Chem. Phys. Lett.* **1990**, *169*, 89−96.
(37) Bo, C.; Sarasa, J.-P.; Poblet, J.-M. *J. Phys. Chem.* **1993**, *97*, 6362−6366.
(38) Macchi, P.; Sironi, A. *Coord. Chem. Rev.* **2003**, *238−239*, 383−412.
(39) Chatt, J.; Duncanson, L. A. *J. Chem. Soc.* **1953**, 2329.

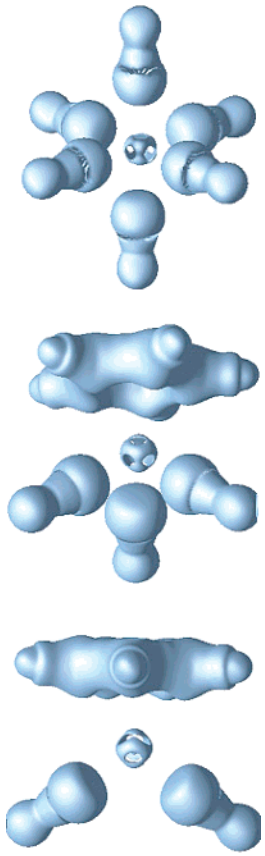

Figure 4. Envelopes for the Laplacian distributions for Mn and the ligands in the complexes $Mn(CO)_6^+$ (top), $CpMn(CO)_3$ (middle), and $CpMn(CO)_2$. The value of $L(\mathbf{r})$ for Mn is the same as above, while for the ligands it is set at zero. The $L(\mathbf{r}) = 0$ surface separates the regions of CC from those of CD. Note in particular the pronounced nonbonded CC on each carbonyl carbon and the manner in which it is directed at a center of CD or hole on Mn. The torus of charge removal bounding the CC on a carbonyl carbon is the Laplacian complement of the π^* orbital. A CC of Mn is directed at the pronounced hole in $L(\mathbf{r})$ found at the center of a Cp ring, thereby aligning the adjacent holes with the Cp ring of charge concentration. Note the increased size of the hole on Mn in the lower diagram that is oppositely directed to the one of almost equal size formed by the removal of a CO from $CpMn(CO)_3$.

to the atomic population on the metal atom. One finds, for example, that only 0.5 of the four electrons in the e_g set resides on Cr in $Cr(CO)_6$, an observation further strengthening the donor−acceptor interpretation of the Cr−C interaction.

$Mn(CO)_6^+$, $CpMn(CO)_3$, and $CpMn(CO)_2$ have the same atomic graph for Mn, and the CDs in the faces of the atomic graph are aligned with the CCs on the ligands in the manner of donor−acceptor interactions. This is illustrated in Figure 4, which displays the Laplacian envelope map for the metal and for the ligands in $Mn(CO)_6^+$, $CpMn(CO)_3$, and $CpMn(CO)_2$. In $Mn(CO)_6^+$ each hole or CD on Mn is aligned with the pronounced nonbonded CC of a carbon in CO. Three of the CDs on Mn in $CpMn(CO)_3$ are aligned with the nonbonded CCs on the carbonyl carbons and the remaining three with the ring of charge concentration associated with the π density of Cp. The association of a Cp ring with three of the faces of the atomic graph is

the structural equivalent of the isolobal replacement of Cp^- with three carbonyls.[29]

The form of the atomic graph persists even when fewer than six formal ligand electron pairs are involved, as in $CpMn(CO)_2$. The CCs of the Cp ring and of the two carbonyl carbons occupy five of the faces of the atomic graph, leaving one face vacant. This vacancy defines the acceptor ability of $CpMn(CO)_2$ and is the site for the addition of the CC of the hydride ion. The position of the vacancy determines the geometry of the adduct. The angle between the CD directed at a carbonyl C and the vacancy is 86° in the reactant $CpMn(CO)_2$, and the same angle after the filling of the vacancy by the hydride ion is 84°. The CCs exceed the values of the CDs in the atomic graph for Mn by a factor ranging from 5 to 20 and are found on average 0.02 au farther from the Mn nucleus. In $Mn(CO)_6^+$, $L(\mathbf{r}) = 37.9$ au at a CC and 2.5 au at a CD. Replacement of three CO ligands with a Cp in $CpMn(CO)_3$ causes a decrease in the average value of $L(\mathbf{r})$ to 36 au and an increase in the value for the CDs to 6.1 au, the latter increase signifying an increased interaction with the σ density of the ligands.

The creation of the vacancy in the atomic graph by the removal of a CO from $CpMn(CO)_3$ increases the average value of $L(\mathbf{r})$ at the CCs to 39 au while reducing the value of $L(\mathbf{r})$ at all of the CDs, to an average value of 2.1 au. The effect is most pronounced for the CD corresponding to the vacancy whose value is reduced to 1.7 au, thereby increasing its susceptibility to nucleophilic addition. A surprising consequence of the creation of the vacancy is the still greater reduction in the value of the CD diagonally opposed to it, to a value that is less than zero, −2.8 au, the two CDs creating an angle subtended at the Mn nucleus of 179°. This diagonally opposed arrangement of holes is accounted for by the form of the LUMO in the $CpMn(CO)_2$ fragment, which Lichtenberger points out is predominantly the metal d_{z^2} orbital, one that is ideally set up to accept the donor orbital.[1] The Laplacian distribution gives physical substance to the form of the LUMO, and the identification of the LUMO with a dz^2 orbital accounts for the double-lobed character of the vacancy.

The addition of Cl_3SiH to the vacancy causes a change in the atomic graph of Mn corresponding to the loss of two CCs. Since the number of edges is simultaneously reduced by two, the number of holes remains the same and the characteristic set becomes [6,10,6]. However, the size of the "vacancy" and its diagonally related hole are increased, Figure 5. The necessity for this increase in size is made clear by the contour diagram of the Laplacian for the adduct in the plane of the bonded ring of Si, Mn, and H nuclei. The vacancy is seen to accommodate both the CC of the hydride that is distorted toward the vacancy and a new CC formed within the basin of the Si atom, a consequence of the transfer of 0.6e to Si on forming the adduct. The new CC that lies within the basin of the Si atom has a value of 0.12 au. While the average value of $L(\mathbf{r})$ for the CCs on Mn remains unchanged, the addition reaction causes a large increase in the average value of $L(\mathbf{r})$ at the sites of charge depletion to 7.8 au. In particular, the partial filling of the vacancy and of its diagonally disposed partner increases their values to 8.7 au, signifying an attendant increase in σ bonding to the ligands. The form of the Laplacian distribution shows clearly the participation of both the Si and H atoms in σ bonding to the Mn atom.

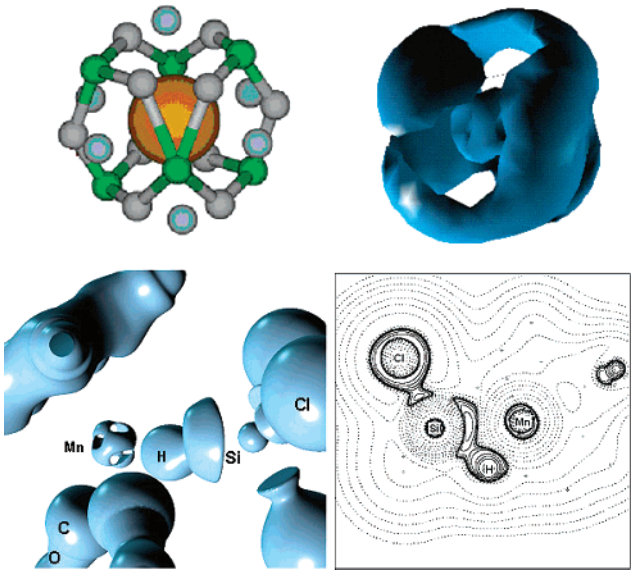

Figure 5. Upper diagrams show the atomic graph and its envelope for Mn in the adduct. Note the large size of the axial faces or regions of charge depletion, one of which serves as the receptor for the CCs from H and Si. The $L(\mathbf{r})$ envelope for the entire molecule shows the CC of the hydridic H and the CC on the valence edge of the Si that are directed at the large vacancy in the atomic graph of Mn. The small sphere by the Si symbol is the CC of its inner core. The final diagram is a contour diagram of $L(\mathbf{r})$ (solid lines denoting regions of charge concentration) to complement the envelope map in delineating the interaction of the CC on the hydridic H and the CC in the valence region of Si with the vacancy in the atomic graph of Mn.

The donor−acceptor interactions defined by the Laplacian distribution of the complexes indicate that the transition metal can act as both a donor and an acceptor, thereby mimicking the properties of the HOMO as well as the LUMO. The Laplacian distribution of Cp has a pronounced hole at the center of the ring, and a CC of the atomic graph of M is directed at this hole, an interaction that leads to the favorable alignment of the three adjacent faces of charge depletion with the ring of charge concentrations associated with the π density of the ring. A similar interaction is found in ferrocene, where the bipyramidal atomic graph of Fe is aligned so that its axial vertexes are directed at the holes in the Cp rings.

More importantly, the donor ability of the metal atom's Laplacian provides a quantifiable measure of the operation of the Chatt−Duncanson $d\pi-p\pi^*$ back-bonding model.[39] The vertexes of the metal's atomic graph are directed at the regions of charge depletion that girdles each CO axis in the vicinity of the C|O interatomic surface. The surface is a pronounced region of charge depletion in the VSCC of C, being the Laplacian equivalent of the π^* LUMO. The resulting transfer of charge to C in the complexes relative to C in free CO ranges from 0.23e in the adduct to 0.32e in $CpMn(CO)_2$. A quantitative demonstration that the transferred charge is localized primarily to a π-like distribution on C is made evident in the increased quadrupole polariza-

tion of C. The quadrupole moment of an axial molecule determines the extent of accumulation of σ-like electron density along the molecular axis, as opposed to its π-like accumulation in a torus about the axis. Because the component parallel to the axis $Q_{\parallel}$(C) and its two perpendicular components $Q_{\perp}$(C), sum to zero, the changes in the parallel or perpendicular components provide a direct determination of the extent of transfer of density between the σ and π systems of a linear molecule. In free CO at the DFT level of theory, there is slight preponderance of the perpendicular (π) over the parallel (σ) components and the magnitude of the atomic moment is small, $|\mathbf{Q}(C)| = 0.18$ au. The change in the quadrupole polarization of CO upon complexation is restricted almost entirely to the increase in the π-like distribution within the basin of the carbon atom, and the resulting changes are dramatic: in $CpMn(CO)_2$ for example, the density transferred to the π-like torus on C, in the amount of 0.32e, causes a 14-fold increase in $|\mathbf{Q}(C)|$ to 2.58 au, with $Q_{\perp}$(C) changing from -0.08 au in free CO to -1.3 au. The values of $|\mathbf{Q}(C)|$ in $CpMn(CO)_3$ and the adduct undergo a corresponding increase to 2.26 au. The carbon atoms in the carbonyl complexes of Cr, Fe, and Ni undergo similar increases in population and in the perpendicular components and magnitude of $\mathbf{Q}$, the increase in $|\mathbf{Q}(C)|$ ranging from 1.3 to 2.3 au.[16] The increase in the magnitude of the perpendicular components of $\mathbf{Q}$ and the associated large increase in $|\mathbf{Q}(C)|$ for a carbon atom in a CO ligand provide an unequivocal and quantifiable demonstration of the operation of the Chatt−Duncanson dπ−pπ* back-bonding model.

Discussion and Conclusions

The question of "where to draw the line?" has an answer in the topology of the electron density, a measurable distribution that determines a molecule's molecular graph: the network of lines of maximum density linking the basins of neighboring atoms and denoting the principal pairwise atomic interactions. This graph is mirrored in the virial graph, the corresponding set of lines demarking the principal interatomic potential energy interactions. The appeal to the physical definition of structure embodied in QTAIM expands one's understanding to include a prediction of possible changes into neighboring structures. The consideration of the structure diagram for a three-membered ring system found in the adduct of $CpMn(CO)_2$ with $HSiCl_3$, in conjunction with the instabilities predicted by the properties of the density at the bond CPs, results in a more complete understanding of the addition reaction.

The bonding defined in the molecular graph is accounted for in terms of the properties of the atoms, in particular their charges and energies and the changes in these quantities incurred during a chemical change. For example, the present results, both structural and in terms of the atomic properties, complement Lichtenberger's description of the reaction of $CpMn(CO)_2$ with $HSiCl_3$ as one leading to the formation of the Mn−H interaction at the expense of a weakening in the Si−H interaction. One now understands that the addition complex, while structurally anchored by the Mn−H bond path, is characterized by a flexible interaction of the $|SiCl_3$ group with the Mn and H atoms of the $CpMn(CO)_2|H|$ group.

The complementary mapping of the regions of charge concentration (CC) and charge depletion (CD) determines the donor−acceptor interactions of transition metal complexes, as displayed by the envelope maps of the Laplacian distributions shown in Figure 4.[16] The Laplacian distribution for the adduct illustrated in Figure 5 demonstrates how the CC $\leftrightarrow$ CD mapping provides a physical complement to models based on frontier orbital arguments. The crystal and ligand field models find expression in the atomic graph of a transition metal atom in the association of its CCs with the orbitals that engage in π but not σ bonding with the ligands, with the roles reversed for its CDs. The donor ability of the metal atom CCs underlies the transfer of π density to the carbonyl carbons as envisaged in the dπ−pπ* back-bonding model, a transfer that is given quantitative physical measure in terms of the changes in the atomic quadrupole polarizations of the carbonyl carbons.

Acknowledgment. We wish to thank Professor D. L. Lichtenberger for the helpful comments provided in his detailed review of the manuscript and Professor Ignacio Vargas-Baca for helpful discussions regarding addition oxidation reactions.

OM049450G